

Valorization of Restaurant Waste Oil Over Cow-bone Doped Siliceous Termite Hills Catalysts Towards Biodiesel Production

Babatunde Esther Olubunmi

University of Ilorin Faculty of Engineering and Technology

Saka H Bamidele

University of Ilorin Faculty of Engineering and Technology

Aderibigbe F Alade

University of Ilorin Faculty of Engineering and Technology

Yusuff Adeyinka

Afe Babalola University

Bisheswar Karmakar

National Institute of Technology Durgapur

Lalthazuala Rokhum

National Institute of Technology Silchar

Gopinath Halder (✉ gopinath_haldar@yahoo.co.in)

National Institute of Technology Durgapur

Research Article

Keywords: Biodiesel, Heterogeneous catalyst, Kinetic studies, Restaurant waste oil, Termite hill

Posted Date: June 14th, 2021

DOI: <https://doi.org/10.21203/rs.3.rs-510139/v1>

License: © ⓘ This work is licensed under a Creative Commons Attribution 4.0 International License.

[Read Full License](#)

1 **Valorization of restaurant waste oil over cow-bone doped siliceous termite hills catalysts**
2 **towards biodiesel production**

3 Babatunde E. Olubunmi¹, Saka H. Bamidele¹, Aderibigbe F. Alade¹, Yusuff Adeyinka².
4 Bisheswar Karmakar³, Lalthazuala Rokhum⁴, Gopinath Halder^{3*}

5 ¹Chemical Engineering Department, Faculty of Engineering, University of Ilorin, Kwara State,
6 P.M.B 1515, Ilorin, Nigeria

7 ²Department of Chemical and Petroleum Engineering, Afe Babalola University, Ado-Ekiti,
8 Nigeria

9 ³Department of Chemical Engineering, National Institute of Technology Durgapur, Durgapur-
10 713209, West Bengal, India

11 ⁴Department of Chemical Engineering, National Institute of Technology Silchar, Silchar 788
12 010, Assam, India

13

14

15

16

17

18 **Corresponding Author:**

19 ***Dr. Gopinath Halder**

20 Professor, Department of Chemical Engineering,

21 National Institute of Technology Durgapur

22 M. G. Avenue, Durgapur- 713209

23 West Bengal, India.

24 Telephone: +91-94347-88189

25 E-mail address: gopinathhaldar@gmail.com

26 **Abstract**

27 Treated termite hill is a potent heterogeneous catalyst in the synthesis of biodiesel from
28 restaurant waste oil (RWO). Two catalysts (raw cow-bone supported on silica; R-SC_{1.5} and
29 calcined cow bone supported on silica; K-SC_{1.5}) were developed and used in biodiesel
30 production. The maximum conversion of RWO was 95.12 % using K-SC_{1.5} at reaction time 2.5
31 h, methanol to oil ratio 9:1, temperature 65°C and catalyst loading of 2 %w/w. The prepared
32 catalysts were characterized using SEM, EDAX, FTIR, XRD and BET analysis. The kinetics of
33 the RWO with R-SC_{1.5} and K-SC_{1.5} was further studied. The E_a and A were found to be 41.4 kJ
34 mol⁻¹, 53.41 kJ mol⁻¹ and 2.24 ×10⁴ min⁻¹, 2.29×10⁶ min⁻¹ respectively. The transesterification
35 reaction adhered to first order law, while physicochemical properties were within ASTM limits.
36 Reusability of K-SC_{1.5} was also examined, which revealed effectiveness up to 5 reuses without
37 significant reduction in biodiesel yield.

38

39

40

41

42 **Keywords:** Biodiesel; Heterogeneous catalyst; Kinetic studies; Restaurant waste oil; Termite
43 hill.

44

45

46

47

48

49

50

51

52

53 **1. Introduction**

54 In the world today, conventional fuels such as natural gas, coal, petroleum etc. are the major
55 sources of energy, however their extensive use has an irreversible impact on the ecosystem
56 through environmental pollution and global warming (Fadhila et al. 2017). Also, these fuels are
57 non-renewable, and at the current rate of use, the tapped reserves are expected to decline
58 critically within 50 years (Babatubde et al. 2020a). These problems prompted the search for
59 substitute fuels which can be sustainably produced and consumed, with the added target of
60 reduced toxic emissions upon combustion that may aid in reversing the climactic damage. These
61 ‘biofuels’, so termed because of their origin from biomass based sources such as plants, animal
62 or algae, have been accumulating research interest for the past few decades. Combined with
63 other renewable sources such as wind, geothermal, hydroelectric, solar etc. the combined energy
64 potential of these largely unused sources is far greater than can be from non-renewable energy
65 sources, with ease of purification and use as well as energy density being the reasons for the
66 latter’s popularity. Biodiesel, being a form of biofuel, is gaining usage in engines and for power
67 generation, yet widespread usage at this point is still largely impractical due to the scattered
68 nature of potential resources. Biodiesel can be synthesized from renewable feedstocks, mainly
69 edible or non-edible vegetable oils. Algae, animal fats, lard, and used oils from restaurants and
70 households are also used as a cost-effective biodiesel feedstock (Dawodu et al. 2014). Polar
71 alcohols (methanol, ethanol) are commonly used in a process known as ‘transesterification’
72 which involves conversion of glycerides or FFAs (free fatty acids) present in the feedstock into
73 esters; however, recent studies by many researchers have shown that less polar alcohols such as
74 2-propanol are more effective in these conversions (Karmakar et al. 2021; Tan et al. 2010).
75 Transesterification is also frequently coupled with esterification, usually as a pre-treatment step
76 for oils that have high amounts of FFAs and are hence unsuitable for alkali-catalyzed conversion
77 due to saponification and hydrolysis (Karmakar and Halder 2019). Here, polar alcohols could
78 convert the FFAs into esters, usually aided by mineral acids that act as a catalyst, and non-polar
79 alcohols are unable to participate in this conversion (Karmakar et al. 2020c). The benefits of
80 biodiesel include biodegradability, high lubricity, low toxicity, high calorific value and high
81 combustion efficacy due to increased oxygen (10 to 11%) and virtually no sulphur. Nevertheless,
82 biodiesel commercialization is hindered by its high total cost of synthesis (Babatunde et al.
83 2020a). For catalyzed conversions, the prime factor that adds into production costs is catalyst

84 preparation cost and recovery or washing, since homogenous catalysts provide high 'one-time;
85 conversions but need to be washed away, typically over multiple rounds, while heterogeneous
86 catalysts face issues of leaching and structural damage hindering their reusability apart from
87 being costly to produce (Karmakar et al. 2018; Karmakar et al. 2020a). Additionally, feedstock
88 procurement and processing (extraction, purification) amount for up to 30% of the total
89 production costs, hence waste oils are a lucrative alternative (Dhawane et. al. 2018; Olutoye and
90 Hammed, 2013). Therefore, there is a need to use low-cost feedstock such as restaurant waste oil
91 (RWO) to reduce the total cost of biodiesel production and also solve the problem of fuel versus
92 food competition (Jung et al. 2018). The Energy Information Administration estimated near 1
93 million gallon of RWO being generated per annum in USA alone. Also, in the EU countries,
94 total RWO production was estimated to be 700,000 - 1,000,000 tons/year (Chhetri et al. 2008).
95 Reports on RWO by several researchers have proven that it is a capable feedstock for biodiesel
96 synthesis (Dhawane et al. 2018; Xiang-nan et al. 2019). Owolabi et al. and Rachael et al.
97 established the efficiency of collected RWO as feedstock for biodiesel synthesis (Owolabi et al.
98 2011; Rachel et al. 2012). Kinetics of RWO transesterification needs to be elucidated for a better
99 insight into its potential for scale-up (Ma et al. 2017). Most kinetic studies on RWO have been
100 performed on processes that use homogeneous acids or bases as catalysts (Dhawane et al. 2018;
101 Jain et al. 2011), however, process kinetics have not been studied by most researchers reporting
102 their works on heterogeneous catalyzed conversions using novel synthetic catalysts.

103 Birla et al. reported the kinetic study of the transesterification of biodiesel from waste cooking
104 oil using snail shell as catalyst (Birla et al. 2012). They found E_a of 79 kJ/mol and A of $2.98 \times$
105 10^{14} min^{-1} . Yusuf et al. reported transesterification kinetics of WCO conversion to biodiesel
106 using anthill-eggshell-Ni-Co mixed oxide catalyst (Yusuf et al. 2017). The E_a and A were found
107 to be 23.99 kJ/mol and $1.62 \times 10^6 \text{ min}^{-1}$ respectively. Comparing this result with Birla et al., it
108 could be stated that the anthill-eggshell-Ni-co mixed oxide catalyst is faster due to lower E_a and
109 A, emphasizing the impact of catalyst nature on process kinetics (Birla et al. 2012; Moradi et al.
110 2015). According to Zhang et al., one way to reduce biodiesel synthesis cost is the full utilization
111 of municipal or agricultural waste resources like cow bone (Ayoola et al. 2018), eggshell (Zabeti
112 et al. 2009), snail shell (Birla et al. 2012; Laskar et al. 2018) as catalysts since they are rich in
113 calcium and when properly activated (Zhang et al. 2010), are very stable with high surface area
114 and porosity, resulting in enhanced catalytic performance. Among the calcium-rich waste

115 materials, cow bone has been selected as the heterogeneous base catalyst as it is abundant in
116 nature, readily available and inexpensive (Birla et al. 2012). Furthermore, the efficiency of this
117 heterogeneous base catalyst could be improved if properly supported on suitable materials.

118 Several heterogeneous base catalysts supports have been utilized ranging from base catalyst
119 supported on carbon material or silica material or alumina material or zeolite material or clay
120 material to metal oxides (Changmai et al. 2020; Hossain et al. 2019; Minh et al. 2019). Although,
121 other supports have also shown to be effective, base catalysts supported on silica have gained
122 more attention for biodiesel production because of its inertness in addition to possessing high
123 surface area and structural stability (Polshettiwar et al. 2009; Samart et al. 2010). Moreover,
124 Farook et al. has documented similar report stating that silica provides ample surface area for any
125 metal to disperse (Ciriminna et al. 2013; Farook et al. 2006). Hence, silica has been widely
126 selected as a support for the base catalyst used in the biodiesel production. Precursors such as
127 rice husk ash (Farook et al. 2006), tetramethoxysilane (TMOS), tetraethoxysilane (TEOS),
128 tetrapropoxysilane (TPOS) (Paulino and Schuchardt 2002), microcrystalline silicon oxide, silica
129 sol, water glass (Shaikh et al. 1993) and termite hill (Ganguli et al. 2013) are excellent sources of
130 silica. Most of these sources are difficult to obtain and/or process, however, termite hills are
131 indigenous to Nigeria and because of this natural abundance as well as their chemical inertness
132 and thermal stability, they have been chosen as a catalyst support of the base catalyst used in this
133 work (Karmakar et al. 2020a). Moreover, termite hill has also been found to contain some oxides
134 and silicates of calcium, iron, aluminium and potassium which are also important catalyst for
135 biodiesel production (Ganguli et al. 2013). A few works such as by Enagbonma et al. and Kumar
136 et al. have reported the use of termite hill as useful sources of bacteria for biofuel production;
137 and except for our previous work (Karmakar et al. 2020a), sufficient literature on the suitability
138 of termite hills as an inert, porous catalyst support for biodiesel synthesis does not exist
139 (Enagbonma et al. 2019; Kumar et al. 2015).

140 For this study, a heterogeneous catalyst was produced using silica derived from termite hill to
141 support CaO rich material. Transesterification of restaurant waste oil occurred in the presence of
142 the prepared catalyst for synthesis of biodiesel. Process parameters such as time, catalyst amount,
143 reaction temperature and methanol to oil ratio were selected as the operating parameters. Kinetic
144 study was carried out. The reaction rate constant (k) and activation energy (E_a) at different

145 temperatures were elucidated. Fuel properties were also tested and equated with the American
146 Standard for Testing Materials (ASTM).

147 **2. Resources and procedure**

148 **2.1. Required materials**

149 The restaurant waste oil (RWO) used as feedstock was obtained from the school restaurant,
150 University of Ilorin, Kwara State, Nigeria. The RWO was preheated to eliminate moisture
151 contents and later filtered to remove impurities. Termite hill abundantly available in the local
152 area of Gidan Kwano, Minna, Nigeria, was selected as the precursor in preparing catalyst support
153 (called silica). The cow-bone was obtained from Saraki abattoir in Ilorin. Methanol (98.9%) and
154 H₂SO₄ (98.9%) were purchased from Sigma-Aldrich in Ilorin. Distilled water was obtained from
155 the Chemical Engineering Laboratory, University of Ilorin.

156 **2.2. Catalyst synthesis**

157 To prepare the support, the termite hill was pulverized into powder. The powder was dissolved
158 in distilled water and mixed thoroughly and left standing for 36 h. After decantation of the
159 excess water, the termite hill was air-dried for 2 days, crushed into powder and dried again in an
160 oven at 120 °C for 2 h to remove residual moisture. The powdered termite hill was sieved using
161 75 µm mesh and kept in a desiccator. Thereafter, powdered 100 g of termite hill was mixed with
162 200 mL aqueous solution of 1M NaOH under gentle agitation at 110 °C for 3 h (Putra et al.
163 2018). Resulting termite hill suspension was filtered and quenched by adding 300 mL ice-cold
164 water, followed by filtration to obtain a silica type phase. Thereafter, it was repeatedly washed
165 with hot distilled water to eliminate impurities as reported by Achyut et al., dried in the oven at
166 80 °C for 30 min and then labeled (S) (Achyut et al. 2010). In the same vein, collected cow-bone
167 was washed, rinsed, dried, and ground into powder using a mechanical grinder, sieved and oven-
168 dried at 110 °C for obtaining a stable weight (called C).

169 To prepare the catalysts, the pretreated cow-bone (C) 1.5 wt % (relative to the weight of support)
170 was added to 10 g silica. The mixture was dissolved in 50 mL water before being placed in an
171 orbital shaker at 200 rpm and kept at 30 °C overnight. Filtration of the solution yields a solid
172 sample (SC_{1.5}), which was dried at room temperature for 24 h and called raw cow-bone

173 supported on silica (R - SC_{1.5}). The R - SC_{1.5} was then calcined at 900 °C for 2 h, and then called
174 calcined cow bone supported on silica (K- SC_{1.5}) and then stored in a desiccator.

175 **2.3. Catalyst Characterization**

176 The prepared catalysts (R - SC_{1.5}. and K - SC_{1.5}) were analyzed to estimate its physical properties
177 such as surface area and pore volume. The analysis was performed using the multi-point BET
178 (Brunauer Emmett Teller) method (Quantachrome instrument version 11.03, NOVA 2200E,
179 Durham, USA). The catalysts were degassed at 196 °C under vacuum for 3 h, which preceded
180 the physical adsorption measurements. The time of analysis was 72.8 min using N₂. A scanning
181 electronic microscopy (SEM) [JEOL, JSM-6510LV, USA] was used to examine the surface
182 morphological structure of the catalysts. The SEM displayed the image of the sample surface at a
183 magnification of 100 μm on a mode of 15 kV average voltages and the elements present on the
184 surface were quantified by using X-ray energy dispersive analysis (EDAX) using OXFORD
185 Instrument INCAX-sight. The X-ray diffraction (XRD), EMPYREAN diffractometer system
186 with CuKα radiation of ($\lambda=1.54060 \text{ \AA}$) at 45 kV, step size of 2θ 0.0260, scanning step time of
187 29.07 seconds and 40 mA between the range of $2\theta = 15.0024$ to 74.9684° was used to determine
188 the chemical phase and the crystalline structure of the functionalized catalyst. The presence of
189 the functional groups was confirmed by using Fourier transform infrared spectrophotometer
190 (Shimadzu FTIR-8400S, Canada) displaying a wave number spectrum between the range of 500
191 cm^{-1} - 4000 cm^{-1} .

192 **2.4. Conversion process**

193 Catalyst performance was examined during transesterification, conducted using a magnetic
194 stirrer hotplate and a 250 mL round bottom flask attached with a condenser and a thermostat to
195 maintain a constant temperature during the reaction. Based on 50 g of RWO, with constant
196 agitation rate of 250 rpm, the reaction took place under the operating conditions of 9:1 methanol
197 to oil ratio, a reaction time of 2.5 h, catalyst loading of 2 wt % (for R- SC_{1.5} and K- SC_{1.5}) and
198 reaction temperatures of 50, 55, 60, and 65 °C. After the reactions, each mixture was poured into
199 separating funnels through filter paper to retain the catalyst for reuse. The filtrate mixture was
200 allowed to separate overnight to obtain a clear layer of biodiesel. The produced biodiesel was
201 collected, purified (through repeated wet—washing and drying) and volumetric fuel yield was

202 calculated using Eq.1. To investigate the quality of the biodiesel synthesized, physico-chemical
203 tests were performed as per ASTM standards.

$$204 \quad \text{Biodiesel Yield (\%)} = \frac{\text{Weight of Biodiesel from RWO}}{\text{Weight of RWO used}} \times 100 \% \quad (1)$$

205 **2.5. Kinetics of transesterification of RWO**

206 For kinetic studies, considered assumptions were:

- 207 1. Methanol concentration is in excess of required stoichiometric ratio and can be considered
208 constant. Thus, the reversible reaction could be ignored as equilibrium is shifted towards
209 product formation (Le Chatelier's principle).
- 210 2. The catalyst efficiently catalyzed every step-wise conversion of the transesterification, and
211 the three consecutive reactions cycles occurred at the same rate as the overall rate of
212 triglyceride conversion (Yusuff et al. 2017),

213 Moreover, Karmakar et al. have also reported that excess methanol is required to avoid the
214 conversion of glyceride while maintaining a forward reaction (Karmakar et al. 2020a).
215 Therefore, the rate law governing the forward reaction of transesterification reaction has been
216 expressed in Eq.2.

$$217 \quad -R_a = \frac{-d[TG_s]}{dt} = k' \cdot [TG] \cdot [MtOH]^3. \quad (2)$$

218 Where $-R_a$ = rate of reaction; TG_s = triglyceride concentration, k' = equilibrium rate constant,
219 $MtOH$ = methanol concentration. Since, the concentration of methanol did not alter the reaction
220 order, it is appropriate to theorize that the reaction adheres to a pseudo-first order reaction.
221 Hence, the Eq.3 has been adapted for the reaction order.

$$222 \quad -R_a = \frac{-d[TG]}{dt} = k \cdot [TG]. \quad (3)$$

223 Where k is modified rate constant, and therefore $k = k'[MtOH]^3$. It has been assumed that at time
224 $t = 0$, the initial concentration of triglycerides was TG_0 mol/dm³, and at time t it falls down to
225 TG_1 . On integrating Eq.3 we have Eq.4, noting that $[TG] = [TG_0](1 - X)$

$$226 \quad -\ln(1 - X) = kt. \quad (4)$$

227 The graph of $-\ln(1 - X)$ against t at different reaction temperatures (50 °C, 55 °C, 60 °C, and 65
228 °C) was plotted to obtain the rate constants at each temperature. Furthermore, to determine the

229 activation energy (E_a , kJ/mol) and the frequency factor (k_a , min⁻¹) of the reaction, the values of
230 the rate constants obtained at different temperatures were plotted against the inverse of
231 temperature.

232 **3. Results and discussion**

233 **3.1. Catalyst characterization**

234 **3.1.1. BET analysis**

235 The BET analysis of both K - SC_{1.5} and R - SC_{1.5} were performed and presented in Table 1. The
236 calcined cow bone supported on silica (K - SC_{1.5}) shows a wider surface area of 440.88 m² g⁻¹ as
237 compared to the raw cow bone supported on silica (R - SC_{1.5}) with surface area of 260.70 m² g⁻¹.
238 This indicates that during the calcination process, the components of the catalyst which tend to
239 hold the particles together have been burnt off thereby increasing the areas to be occupied by the
240 active sites. Furthermore, Birla et al. reported that a higher pore size of a catalyst is necessary as
241 it allows proper diffusion of reactants into the active site of the catalyst (Birla et al. 2012). In
242 this work, the pore size of K - SC_{1.5} (22.90 nm) was larger than R - SC_{1.5} (21.24 nm), hence, this
243 allowed sufficient interactions between the catalyst, reactants and product molecules. The
244 concentration of basic site of the catalyst was also investigated and the value of the R - SC_{1.5}
245 (9.40 mmol/g cat) was found to be lesser than K - SC_{1.5} (10.90 mmol/g cat), this result could be
246 attributed to the oxides of calcium and other basic compounds as reported by Yusuff et al.
247 Furthermore, it also indicates that Lewis base site contributed to high catalyst activity (Yusuff et
248 al. 2017).

249 **3.1.2. Morphological analysis**

250 SEM studies in Fig. 1 shows the structural nature of the raw and calcined catalyst developed
251 respectively. Fig. 1a revealed that the catalyst particles (X) of R - SC_{1.5} are agglomerated and
252 heterogeneous. It possesses coarse and irregularly sized particles with smooth edges. This result
253 is congruent to reports from Mitaphonna et al. when they stated that catalyst particles formed
254 with uncalcined cow bone could be coarse and possess aggregate structure with smaller surface
255 area (Mitaphonna et al. 2019). However, Fig. 1b obviously reveals a deviation in particle size
256 (Y) after calcination (Kusuma and Chandrappa 2019). The particles tend to be dispersed and
257 reduced in size with higher surface area. This indicates that the organic compounds in the K-

258 SC_{1.5} have undergone decomposition, while the inorganic compounds have been converted to
259 their oxides (Ganguli et al. 2013; Mitaphonna et al. 2019). The irregular sized particles tend to
260 have rough edges (Y) which is expected to enhance adequate interaction between the reactants.
261 This result is also congruent to BET results from other studies (Babatunde et al. 2020a).

262 **3.1.3. EDAX analysis**

263 As shown in Fig. 2, the EDAX analysis reveals the elemental compositions of the R-SC_{1.5} and K-
264 SC_{1.5} respectively. The presence of silicon (Si) aluminium (Al), iron (Fe), zinc (Zn) and titanium
265 (Ti) in the two catalysts was due to the natural composition of termite hill (as explained by
266 Ganguli et al.), while the calcium (Ca) was impregnated from cow bone (Ganguli et al. 2013;
267 Nisar et al. 2017). The R - SC_{1.5} contains 63.1 % Si, 17.9 % Ca and 5.1 % K while K-SC_{1.5} has a
268 higher percentage composition of 65.85 %, Si, 21.99 %, Ca and 6.9 % K. The results from the
269 EDAX indicate that the calcination process had a notable effect on the catalyst composition
270 (Farooq et al. 2015; Figueiredo et al. 2010). However, the reverse is seen for aluminium (Al),
271 iron (Fe), zinc (Zn), magnesium (Mg) and titanium (Ti) where their compositions were shown to
272 be higher in R - SC_{1.5} than K - SC_{1.5}. These elements may have also enhanced the catalytic
273 performance of R - SC_{1.5} during the transesterification reaction even without calcination. Lastly,
274 a slight change was also noticed in the percentage composition of sodium (from 2.07 % to 1.73
275 %) and aluminium (from 0.13 % - 0.07 %) between the two catalysts. Also, Table 2 shows the
276 chemical composition of the calcined cow bone as determined by XRF analysis. It reveals the
277 presence of CaO (62.81%) and P₂O₅ (35.4%) and other compounds in lower quantity. The result
278 implies that cow bone is a suitable source of catalyst for biodiesel production. The reported work
279 by Nisar et al. shows good agreement with the findings reported in this study (Nisar et al. 2017).
280 Moreover, the cow bone contains Fe₂O₃ (0.45 %), CuO (0.004 %), ZnO (0.015 %), SrO (0.161
281 %), CeO₂ (0.071 %), K₂O (0.25 %) and Li₂O (0.839 %) at very low percentages. Even at lower
282 percentage, they could also have contributed to the catalyst reactivity. This further confirmed the
283 results obtained from the EDAX analysis.

284 **3.1.4. Spectral analysis**

285 The X-ray diffraction analysis of the K-SC_{1.5} was further investigated to determine the size and
286 crystallinity of the synthesized material. As shown in Fig. 3, 2 θ values from 15°-75° reveal the
287 nature and crystallinity of the materials. The peaks at 32.49° and 53.62° indicates the presence of

288 SiO₂ (quartz) in the form of a rhombohedra crystal. The peaks at 34.12°, 47.11°, 63.97°, 68.11°,
289 and 69.24° also indicate the presence of CaO in the form of the cubic crystal system (Farooq et
290 al. 2015). Hence, the XRD analysis revealed the presence of two prominent crystalline phases
291 derived from silicon oxide (SiO₂) and calcium oxide (CaO) (Lesbani et al. 2013). The traces of
292 these compounds were also confirmed by elemental analysis. Presence of other compounds may
293 be confirmed from other non-major peaks in the spectrum.

294 As depicted in Fig. 4, the FTIR spectrum of K-SC_{1.5} was also investigated. The wavenumber
295 between 3400 cm⁻¹ and 3650 cm⁻¹ represents symmetric and asymmetric -OH stretching of H-
296 bonded water which could be as a result of moisture adsorption or the presence of Ca(OH)₂ in
297 trace amounts (Varadwaj et al. 2013). The wavenumber 1600 cm⁻¹ also revealed an H-O-H
298 bending vibration of coordinated water molecules present in the interlayer structure. The
299 wavenumbers 1428.39 cm⁻¹ and 931.34 cm⁻¹ can be correlated to stretching vibrations of CO₃²⁻
300 groups, in CaCO₃ (Lesbani et al. 2013). According to Varadwaj et al., the absorption band at
301 wavenumber 578.14 cm⁻¹ also suggested the presence of Ca-O as reported by (Varadwaj et al.
302 2013). Furthermore, the absorption spectrum at wavenumber 1096.11cm⁻¹ suggested the
303 presence of silicate ion (Si-O stretch) as a functional group in the material (Yusuff et al. 2017).
304 The presence of all these stretches and vibration bonds may have been responsible for the high
305 reactivity of the calcined catalyst (K-SC_{1.5}).

306 Furthermore, FTIR of the biodiesel produced using K - SC_{1.5} at 65 °C under the stated conditions
307 was examined. The spectrum in Fig. 5 shows the absorption band at wavenumber 3417.11 cm⁻¹,
308 suggesting that the O-H stretching vibration may represent alcohols. The band of 1735.24 cm⁻¹
309 suggests the vibration of double bonds stretching of ester carbonyl group of triglycerides (C=O
310 stretch) which may be due to the presence of methyl esters. Other bands seen were at wave
311 numbers 1450.5cm⁻¹, 1393.97cm⁻¹, and 749.23cm⁻¹ which may also depict the presence of C-O
312 ester groups (Yusuff et al. 2018).

313 **3.2. Transesterification**

314 Reactions were conducted in the presence of R-SC_{1.5} and K-SC_{1.5} under the operating conditions
315 of 9:1 (methanol to RWO ratio), reaction time of 2.5 h, catalyst loading of 2 wt % relative to
316 RWO and reaction temperatures of 50, 55, 60, and 65 °C (Adepoju et al. 2020; Nisar et al. 2017).
317 The temperature was varied between 50-65°C so as to investigate the kinetics of the reaction. In

318 Fig. 6, the RWO conversion tends to increase as the reaction temperature increases. The
319 maximum yields attained by R-SC_{1.5} and K-SC_{1.5} were 68.1% and 95.12% respectively. Hence, it
320 is worthy of note to state that the higher conversion attained by K- SC_{1.5} was due to the influence
321 of calcination on the catalyst (Farooq et al. 2015).

322 **3.3. Fuel properties**

323 Physicochemical properties of the FAMEs obtained using K-SC_{1.5} as catalyst was examined and
324 compared with values set by the American Standard for Testing Materials (ASTM). The results
325 are congruent with reports from Chinyere et al. as shown in Table 3, where the values were
326 found to be within required range (Chinyere et al. 2017). High flash point and fire point specify
327 transportation and fuel storage efficiency. Substantial improvement in calorific value was
328 observed which implies that the fuel is energy efficient. Since increased fuel viscosity results
329 inefficient atomization due to low lubricity, the low kinematic viscosity observed in the fuel is
330 responsible for improved performance. The delay in a fuel's ignition can be measured by cetane
331 number of the obtained product. The API gravity value obtained (39.61) also confirmed that the
332 RWO-biodiesel is less dense relative to the density of water (Karmakar et al. 2020a).

333 **3.4. RWO transesterification kinetics**

334 The influence of temperature and time (using R-SC_{1.5}) on RWO conversion is revealed in Fig.
335 7a. Although the conversion of RWO remains low compared to K-SC_{1.5}, the R-SC_{1.5} could show
336 potential towards higher conversion of RWO in further studies. The influences of temperature
337 and time (using K-SC_{1.5}) on RWO conversion is revealed in Fig. 7b. The effect of increasing the
338 reaction temperature between 50 °C and 55 °C was obvious even as time increases from 30 min
339 to 60 min. Also, the conversions curve tends to intersect each other between the reaction
340 temperatures 55 °C – 60 °C. However, as time and temperature increase, the curves tend to split.
341 This commensurate with reports from literature, as increase in temperature allows the mass
342 transfer and proper dispersion of catalyst molecules.

343 **3.4.1. Determining E_a and A**

344 In order to deduce the kinetic parameters, $-\ln(1-x)$ was plotted against t as shown in Fig. 8 and
345 the correlation coefficients were >0.9 for both catalysts. As shown in Fig. 9, the E_a and A were
346 41.4 kJ/mol and $2.24 \times 10^4 \text{ min}^{-1}$ for R-SC_{1.5} and 53.41 kJ/mol and $2.29 \times 10^6 \text{ min}^{-1}$ for K-SC_{1.5}

347 respectively. These were determined by plotting $\ln(k)$ of rate constants for each temperature
348 against the inverse of reaction temperatures ($1/T$). In this plot, the R-squared values for R-SC_{1.5}
349 and K-SC₁ were found to be 0.9501 and 0.9959 respectively. The result was in agreement with
350 reported works as the range of E_a observed in literature were mostly amid 33-84 kJ/mol
351 (Deshmane and Adewuyi 2013; Feyzi and Shahbazi 2017). E_a values vary depending on process,
352 feedstock and catalyst type (Endalew et al. 2011). Krishnamurthy et al. reported an E_a of 67.21
353 kJ/mol and A of $5.182 \times 10^8 \text{ min}^{-1}$ from the transesterification of scum oil (Krishnamurthy et al.
354 2020). Furthermore, Birla et al. documented activation energy of 79 KJ/mol and $2.98 \times 10^{10} \text{ min}^{-1}$
355 ¹ in converting waste cooking oil through a heterogeneous catalyst (Birla et al. 2012).

356 **3.4.2. Reusability of K-SC_{1.5}**

357 The reusability tests aimed at establishing the extent of leaching were carried out when the first
358 cycle of transesterification reaction was completed. The test was conducted for 5 consecutive
359 cycles under reaction conditions discussed earlier in this study. After completion of the reaction,
360 filtration ensured recovery of the catalyst, and a subsequent wash using methanol. The
361 conversion remains stable for the first three cycles and reaches 90.45 % at the end of the 5th
362 cycle as shown in Fig. 10. The decrease in the yield of methyl ester is from the blockage of
363 active catalytic sites in the support structure, along with loss of active metals from the catalyst
364 due to leaching. This was in agreement with literature reports from Olutoye and Hameed,
365 Adepoju et al. and by Karmakar et al. in their works with acid and base doped carbonaceous
366 supports (Adepoju et al. 2020; Karmakar et al. 2020a; Karmakar et al. 2020b; Karmakar et al.
367 2020c; Karmakar et al. 2021; Olutoye and Hameed 2013).

368 **4. Conclusion**

369 In this study, we investigated biodiesel synthesis from restaurant waste oil (RWO) with R-SC_{1.5}
370 and K-SC_{1.5} as heterogeneous catalysts. The K-SC_{1.5} was found to give maximum biodiesel
371 conversion of 95.12 % and fuel properties were found to be within ASTM limits. Also, based on
372 maximum percentage conversion and information deduced from various characterizations such
373 as SEM, FTIR, XRD, and EDAX, the kinetic studies of the restaurant waste oil was studied
374 using K-SC_{1.5}. The E_a and A were found to be 53.41 kJ/mol and $2.29 \times 10^6 \text{ min}^{-1}$ respectively,
375 which is congruent with most results reported in available literature. Hence, it could be stated
376 that treated termite hill is a recommendable catalyst for the transesterification of RWO since it

377 reduces the total cost of biodiesel production and can also help promote the commercialization of
378 biodiesel.

379 **Ethics approval and consent to participate**

380 Not applicable

381 **Consent for publication**

382 Not applicable

383 **Availability of data and materials**

384 All data generated or analyzed during this study are included in this article.

385 **Competing interests**

386 The authors declare that they have no competing interests.

387 **Funding**

388 No financial aid from any commercial or public agency was received towards completion of this
389 research.

390 **Authors' contributions**

391 **BEO** conceptualized the study and listed necessary resources. **BK** and **BEO** handled software
392 based experimental designing and formal analysis as well as data curation. They also wrote the
393 original draft. **SHB**, **AFA** and **YA** were the experimental investigators who also validated
394 obtained data, while **GH** was the supervisor and was in charge of this project. **BK**, **LR** and **GH**
395 took the responsibility of reviewing and editing the manuscript. **GH** handled submission related
396 procedures. The final version of the manuscript was read and approved by all authors.

397 **Acknowledgements**

398 The authors express their sincere gratitude to the technologists at the Department of Chemical
399 Engineering, University of Ilorin and Federal University of Technology Minna, Nigeria for their
400 immense support during execution of the work.

401 **References**

402 Achyut KP, Mishra BG, Mishra DK, Singh RK (2010) Effect of sulphuric acid treatment on the
403 physiochemical characteristics of kaolin clay. *Coll Surf A: Phys Eng Asp* 363(1-3):98-104.
404 <https://doi.org/10.1016/j.colsurfa.2010.04.022>

405 Adepoju TF, Ibeh MA, Babatunde EO, Abegunde GS, Adepoju PO, Asuquo AJ, Osueke CO
406 (2020) Datasets on process transesterification of binary blend of oil for fatty acid ethyl ester
407 (FAEE) synthesized via the ethanolsis of heterogeneous doped catalyst. *Data Brief* 31:105905.
408 <https://doi.org/10.1016/j.dib.2020.105905>

409 Ayoola AA, Igho EB, Babalola R, Ojewumi EM, Ajibola O, Oluwabunmi GA, Fayomi SO
410 (2018) Production of biodiesel from soyabean oil using calcium oxide and cowbone as catalysts.
411 *Mater Focus* 7(4):542-548. <https://doi.org/10.1166/mat.2018.1530>

412 Babatunde EO, Karmakar B, Aderemi OM, Akpan UG, Auta M, Halder G (2020a) Parametric
413 optimization by Taguchi L9 approach towards biodiesel production from restaurant waste oil
414 using Fe-supported anthill catalyst. *J Env Chem Eng* 6:104288.
415 <https://doi.org/10.1016/j.jece.2020.104288>

416 Babatunde EO, Saka HB, Olutoye MA, Akpan UG, Auta M (2020b) Synthesis of fatty acid
417 methyl ester from used vegetable oil using activated anthill as catalyst. *Niger J Tech* 39(1):140-
418 147. <http://dx.doi.org/10.4314/njt.v39i1.15>

419 Birla A, Singh B, Upadhyay SN, Sharma YC (2012) Kinetics studies of synthesis of biodiesel
420 from waste frying oil using a heterogeneous catalyst derived from snail shell. *Biores Tech*
421 106:95–100. <https://doi.org/10.1016/j.biortech.2011.11.065>

422 Changmai B, Vanlalveni C, Ingle AP, Bhagat R, Rokhum L (2020) Widely used catalysts in
423 biodiesel production: A review. *RSC Adv* 10:41625-41679.
424 <https://doi.org/10.1039/D0RA07931F>

425 Chhetri AB, Watts KC, Islam MR (2008) Waste cooking oil as an alternate feedstock for
426 biodiesel production. *Energies*, 1(1):3-18. <https://doi.org/10.3390/en1010003>

427 Chinyere BE, Callistus NU, Okechuckwu DO (2017) Optimization of the methanolysis of lard
428 oil in the production of biodiesel with response surface methodology *Egypt J Pet* 26(4):1001–
429 1011. <https://doi.org/10.1016/j.ejpe.2016.12.004>

430 Ciriminna R, Fidalgo A, Pandarus V, Beland F, Iiharco LM, Pagliaro M (2013) The sol-gel route
431 to advance silica-based materials and recent applications. Chem Rev 113(8):6592-6620.
432 <https://doi.org/10.1021/cr300399c>

433 Dawodu FA, Ayodele O, Xin J, Zhang S, Yan D (2014) Effective conversion of non-edible oil
434 with high free fatty acid into biodiesel by sulphonated carbon catalyst. Appl. Energy 114:819-
435 826. <http://dx.doi.org/10.1016/j.apenergy.2013.10.004>

436 Deshmane VG, Adewuyi YG (2013) Synthesis and kinetics of biodiesel formation via calcium
437 methoxide base catalyzed transesterification reaction in the absence and presence of ultrasound.
438 Fuel 107:474-482. <http://dx.doi.org/10.1016/j.fuel.2012.12.080>

439 Dhawane SH, Karmakar B, Ghosh S, Halder G (2018) Parametric optimization of biodiesel
440 synthesis from waste cooking oil via Taguchi approach. J Env Chem Eng 6:3971-3980.
441 <https://doi.org/10.1016/j.jece.2018.05.053>

442 Enagbonma BJ, Babalola OO (2019) Environmental sustainability: A review of termite mound
443 soil material and its bacteria. Sustainability 11(14):38-47. <https://doi.org/10.3390/su11143847>

444 Endalew AK, Kiros Y, Zanzi R (2011) Inorganic heterogeneous catalysts for biodiesel
445 production from vegetable oils. Biomass Bioener 35:3787-3809.

446 Fadhila BB, Emaad TBA, Albadreeb MA (2017) Biodiesel production from mixed non-edible
447 oils, castor seed oil and waste fish oil. Fuel 210:721-728.
448 <https://doi.org/10.1016/j.fuel.2017.09.009>

449 Farook A, Balakrishnan S, Wong P (2006) Rice husk ash silica as a support material for
450 ruthenium based heterogeneous catalyst. J Phys Sci 17(2):1-13.

451 Farooq M, Ramli A, Naeem A (2015) Biodiesel production from low FFA waste cooking oil
452 using heterogeneous catalyst derived from chicken bones. Renew Energy, 76:362-368.
453 <https://doi.org/10.1016/j.renene.2014.11.042>

454 Feyzi M, Shahbazi Z (2017) Preparation, kinetic and thermodynamic studies of Al-Sr
455 nanocatalysts for biodiesel production. J Taiwan Inst Chem Eng 71:145-155.
456 <https://doi.org/10.1016/j.jtice.2016.11.023>

457 Figueiredo M, Fernando A, Martins G, Freitas J (2010) Effect of the calcination temperature on
458 the composition and microstructure of hydroxyapatite derived from human and animal bone.
459 Ceram Int 36(8):2383-2393. <https://doi:10.1016/j.ceramint.2010.07.016>

460 Ganguli AK, Kumar S, Baruah A, Vaidya S (2013) Nanocrystalline silica from termite mounds.
461 Curr Sci 106(1):83-88.

462 Hossain MN, Siddik Bhuyan MSU, Md Ashraful Alam AH, Seo YC (2019) Optimization of
463 biodiesel production from waste cooking oil using S-TiO₂/SBA-15 heterogeneous acid catalyst.
464 Catalysts 9(1):67. <https://doi.org/10.3390/catal9010067>

465 [Jain S, Sharma MP, Rajvanshi S \(2011\) Acid base catalyzed transesterification kinetics of waste](#)
466 [cooking oil. Fuel Proc Tech 92\(1\):32-38. https://doi.org/10.1016/j.fuproc.2010.08.017](#)

467 Jung J, Ohb J, Baekc K, Leed J, Kwona EE (2018) Biodiesel production from waste cooking oil
468 using biochar derived from chicken manure as a porous media and catalyst. Energy Conv
469 Manage, 165:628-633. <https://doi.org/10.1016/j.enconman.2018.03.096>

470 Karmakar B, Dhawane SH, Halder G (2018) Optimization of biodiesel production from castor
471 oil by Taguchi design. J Env Chem Eng 6:2684-2695. <https://doi.org/10.1016/j.jece.2018.04.019>

472 Karmakar B, Ghosh B, Samanta S, Halder G (2020a) Sulfonated catalytic esterification of
473 *Madhuca indica* oil using waste Delonix regia: L16 Taguchi optimization and kinetics. Sust
474 Energy Tech Assess 37:100568. <https://doi.org/10.1016/j.seta.2019.100568>

475 [Karmakar B, Ghosh B, Halder G \(2020b\) Sulfonated *Mesua ferrea* linn seed shell catalyzed](#)
476 [biodiesel synthesis from castor oil – Response surface optimization. Front Energy Res 8:576792.](#)
477 <https://doi.org/10.3389/fenrg.2020.576792>

478 Karmakar B and Halder G (2019) Progress and future of biodiesel synthesis: Advancements in
479 oil extraction and conversion technologies. Energy Conv Manage 182:307-339.
480 <https://doi.org/10.1016/j.enconman.2018.12.066>

481 [Karmakar B, Hossain A, Jha B, Sagar R, Halder G. \(2021\) Factorial optimization of biodiesel](#)
482 [synthesis from castor-karanja oil blend with methanol-isopropanol mixture through acid/base](#)
483 [doped *Delonix regia* heterogeneous catalysis. Fuel 285:119197.](#)
484 <https://doi.org/10.1016/j.fuel.2020.119197>

485 [Karmakar B, Samanta S, Halder G \(2020c\)](#) Delonix regia heterogeneous catalyzed two-step
486 biodiesel production from Pongamia pinnata oil using methanol and 2-propanol. J Clean Prod
487 255:120313. <https://doi.org/10.1016/j.jclepro.2020.120313>

488 Krishnamurthy KN, Sridhara SN, Ananda K (2020) Optimization and kinetic study of biodiesel
489 production from *Hydnocarpus wightiana* oil and diary waste scum CaO nano catalyst. Renew
490 Energy 146:280-296. <https://doi.org/10.1016/j.renene.2019.06.161>

491 Kumar M and Sharma MP (2015) Assessment of potential of oils for biodiesel production.
492 Renew Sust Energy Rev 44:814–823. <https://doi.org/10.1016/j.rser.2015.01.013>

493 Kusuma M and Chandrappa GT (2019) Effect of calcination temperature on characteristic
494 properties of CaMoO₄ nanoparticles. J Sci Adv Mater Dev 4(1):150-157.
495 <https://doi.org/10.1016/j.jsamd.2019.02.003>

496 [Laskar IB, Rajkumari K, Gupta R, Chatterjee S, Paul B, Rokhum, L \(2018\)](#) Waste snail shell
497 [derived heterogeneous catalyst for biodiesel production for the transesterification of soybean](#)
498 [oil. RSC Adv, 8:20131-20142. https://doi.org/10.1039/c8ra02397b](#)

499 Lesbani A, Tamba P, Mohadi R, Fahmariyanti (2013) Preparation of calcium oxide from
500 Achatina fulica as catalyst for production of biodiesel from waste cooking oil. Indones J Chem
501 13(2):176-180.

502 Ma Y, Wang Q, Sun X, Wu C, Gao Z (2017) Kinetic studies of biodiesel production from waste
503 cooking oil using FeCl₃-modified resin as heterogeneous catalyst. Renew Energy 107:522-530.
504 <https://doi.org/10.1016/j.renene.2017.02.007>

505 Minh ACL, Quitainb AT, Lama MK, Yusupa S, Sasakid M, Kidab T (2019) Development of
506 high microwave-absorptive bifunctional graphene oxide based catalyst for biodiesel production.
507 Energy Conv Manage 180:1013-1025. <https://doi.org/10.1016/j.enconman.2018.11.043>

508 Mitaphonna R, Ramli M, Maulana I, Novita D, Zahara I, Wardani R (2019) Preparation of
509 heterogenous catalyst of aceh cow bone material and its catalytic performance for biodiesel
510 synthesis. Int Proc Asia Youth Conf 2599-2643. <https://doi:10.5281/zenodo.2549060>

511 Moradi GR, Mohadesi M, Ghanbari M, Moradi MJ, Hosseini SH, Davoodbeygi Y (2015)
512 Kinetic comparison of two basic heterogeneous catalysts obtained from sustainable resources for
513 transesterification of waste cooking oil. Biofuel Res J 6:236-241.

514 Nisar J, Razaq R, Farooq M, Iqbal M, Khan RA, Sayed M, Rahman I (2017) Enhanced biodiesel
515 production from Jatropha oil using calcined waste animal bones as catalyst. *Renew Energy*
516 101:111–119. <https://doi.org/10.1016/j.renene.2016.08.048>

517 Olutoye MA and Hammed BH (2013) A highly active clay-based catalyst for the Synthesis of
518 fatty acid methyl ester from waste cooking palm oil. *Appl Cat A* 450:57-62.
519 <https://doi.org/10.1016/j.apcata.2012.09.049>

520 Owolabi RU, Osiyemi NA, Amosa MK, Ojewumi ME (2011) Biodiesel from
521 household/restaurant waste cooking oil (WCO). *J Chem Eng Proc Tech* 2(4):1-4
522 <https://doi.org/10.4172/2157-7048.1000112>

523 Paulino I and Schuchardt U (2002) Studies of MCM-41 obtained from different sources of silica.
524 *Stud Surf Sci Catal* 141:93-100. [https://doi.org/10.1016/S0167-2991\(02\)80529-8](https://doi.org/10.1016/S0167-2991(02)80529-8)

525 Polshettiwar V, Len C, Fihri A (2009) Silica-supported palladium: Sustainable catalysts for cross
526 coupling reactions. *Coord Chem Rev* 253(21-22):2599-2626
527 <https://doi.org/10.1016/j.ccr.2009.06.001>

528 Putra DM, Irawan P, Ristianingsih Y, Nata IF (2018) A cleaner process of biodiesel production
529 from waste cooking oil using materials as a heterogeneous catalyst and its kinetic study. *J Clean*
530 *Prod* 195:1249-1258. <https://doi.org/10.1016/j.jclepro.2018.06.010>

531 Rachael W and Denise B (2012) An investigation of restaurant waste oil characteristics for
532 biodiesel production in Trinidad and Tobago. *Energy Sustain Dev* 16(4):515-519.
533 <https://doi.org/10.1016/j.esd.2012.05.005>

534 Samart C, Chaiya C, Reubroycharoen P (2010) Biodiesel production by methanolysis of
535 soyabean oil using calcium supported on mesosilica catalyst. *Energy Conv Manag* 51(7):1428-
536 1431. <https://doi.org/10.1016/j.enconman.2010.01.017>

537 Shaikh, AA, Joshi PN, Jacob NE, Shiralkar VP (1993) Direct hydrothermal crystallization of
538 high- silica large-pore mordenite. *Zeolites* 13(2):511-517. [https://doi.org/10.1016/0144-
539 2449\(93\)90227-T](https://doi.org/10.1016/0144-2449(93)90227-T)

540 Tangboriboon N, Kunanuruksapong A, Sirivat A (2012) Preparation and properties of calcium
541 oxide from eggshells via calcination. *Mater Science Poland* 30(4):313-322.
542 <https://doi.org/10.2478/s13536-012-0055-7>

543 Tan KT, Gui MM, Lee KT, Mohamed AR (2010) An optimization study of methanol and ethanol
544 in supercritical alcohol technology for biodiesel production. *J Supercrit Fluids* 53(1-3):82-87.
545 <https://doi:10.1016/j.supflu.2009.12.017>

546 Varadwaj GBB, Rana S, Parida KM (2013) Amine functionalized K10 montmorillonite: a solid
547 acid base catalyst for the knoevenagel condensation reaction. *Dalton Trans* 42(14):5122-5129.
548 <https://doi.org/10.1039/C3DT32495H>

549 Xiang-nan Z, Xian-jun L, Qiang W, Jun Q, Sha-sha W, Xin-yu L, Lin L (2019) Clean utilization
550 of waste oil: Soap collectors prepared by alkaline hydrolysis for fluorite flotation. *J Clean Prod*
551 240:118179. <https://doi.org/10.1016/j.jclepro.2019.118179>

552 Yusuff AS, Adeniyi OD, Azeez SO, Olutoye MA, Akpan UG (2018) Synthesis and
553 characterization of anthill-eggshell-Ni-Co mixed oxides composite catalyst for biodiesel
554 production from waste frying oil. *Biofuel Bioprod Bioref* 13(1):37-47.
555 <https://doi.org/10.1002/bbb.1914>

556 Yusuff AS, Adeniyi OD, Olutoye MA, Akpan UG (2017) Kinetic study of transesterification of
557 waste frying oil to biodiesel using anthill-eggshell-Ni-Co mixed oxide composite catalyst. *Pet*
558 *Coal* 60(1):157–167. Available at: <https://www.researchgate.net/publication/324834185>

559 Zabeti M, Daud WMAW, Mohamed KA (2009) Activity of solid catalysts for biodiesel
560 production: A review. *Fuel Proc Tech* 90(6):770-777.
561 <https://doi.org/10.1016/j.fuproc.2009.03.010>

562 Zhang J, Chen S, Yang R, Yan J (2010) Biodiesel production from vegetable oil using
563 heterogeneous acid alkali catalyst. *Fuel* 89(10):2939-2944.
564 <https://doi.org/10.1016/j.fuel.2010.05.009>

565

Figures

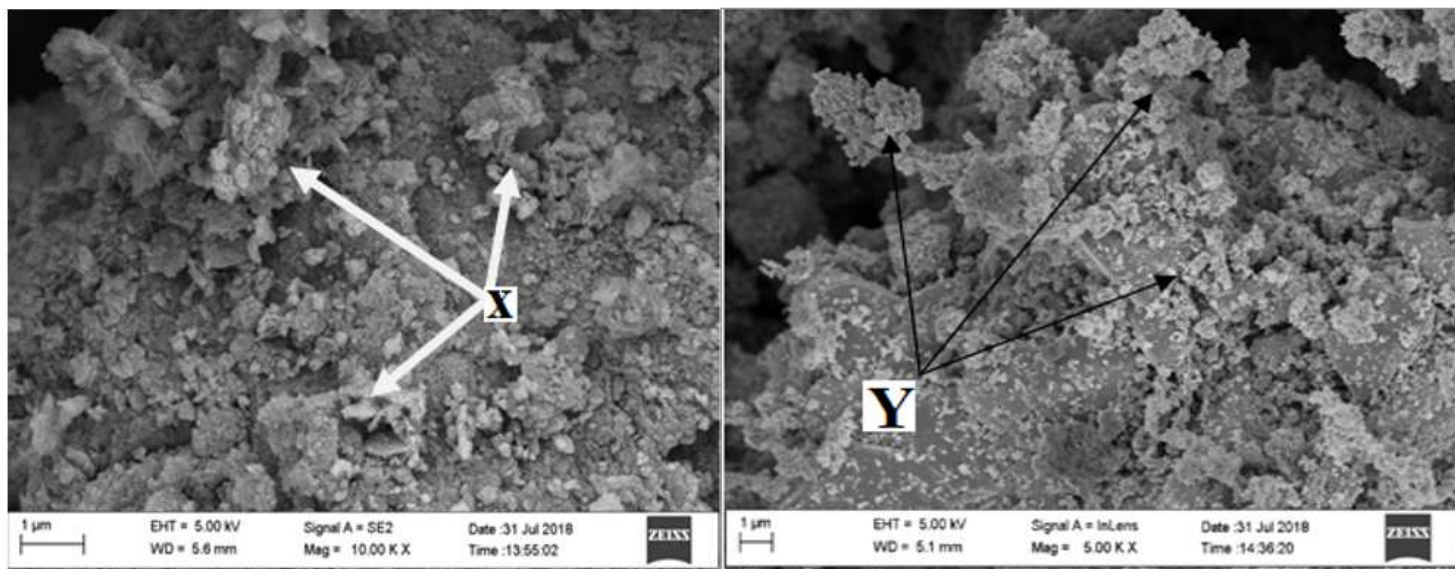


Figure 1

SEM Image of (a) R - SC1.5 and (b) K- - SC1.5

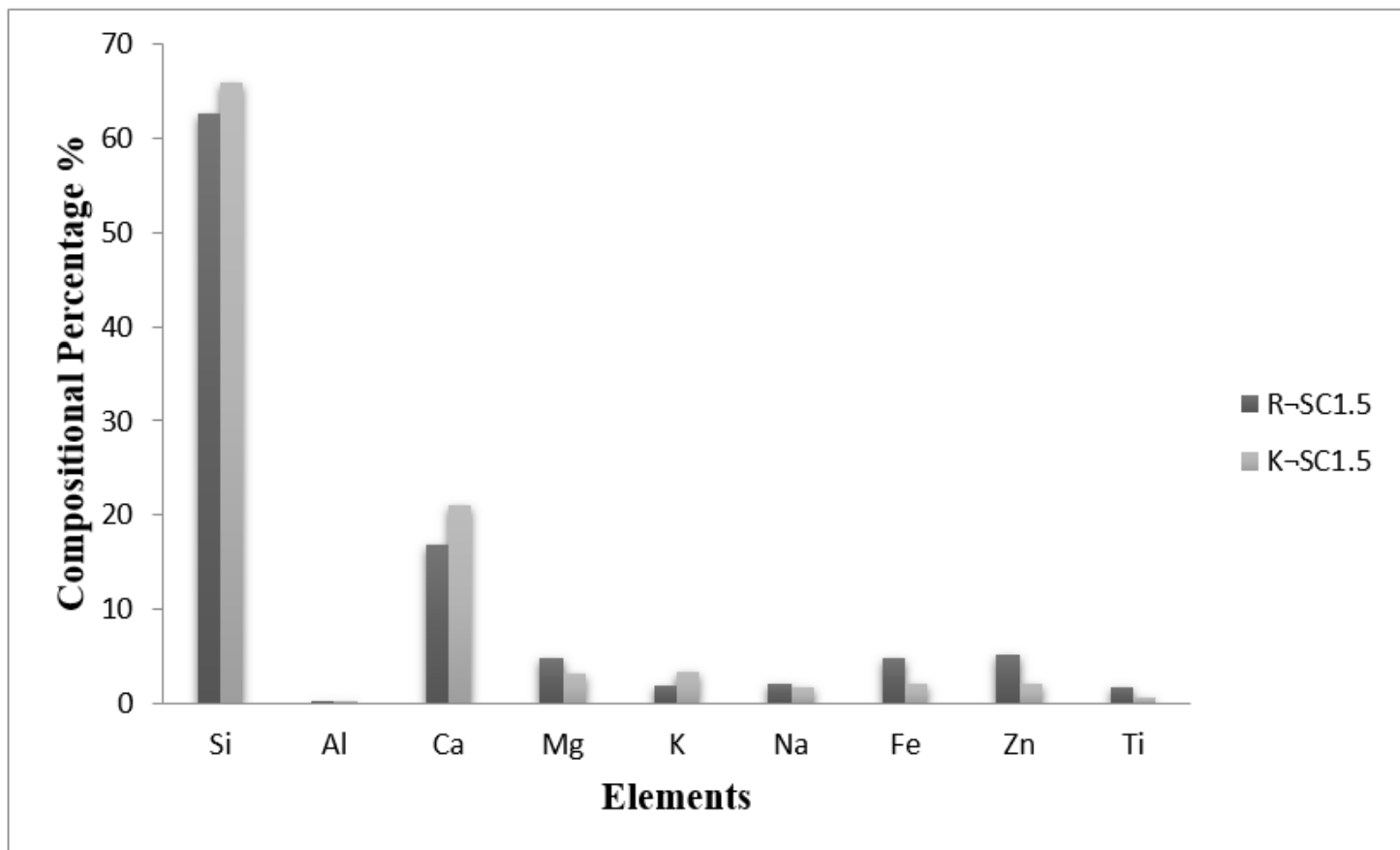


Figure 2

EDX analysis of the R - SC1.5 and K- - SC1.5

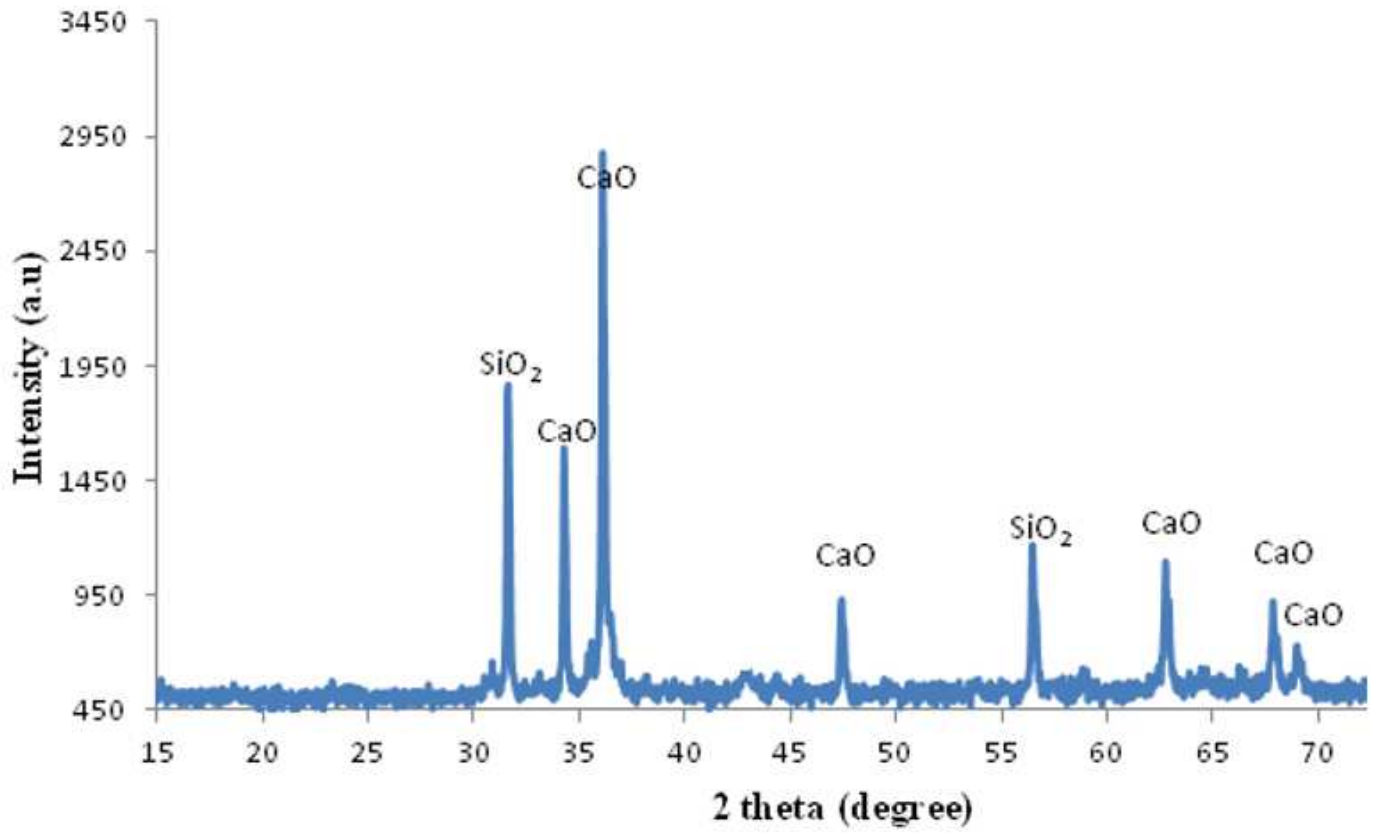


Figure 3

XRD Spectrum of K- - SC1.5

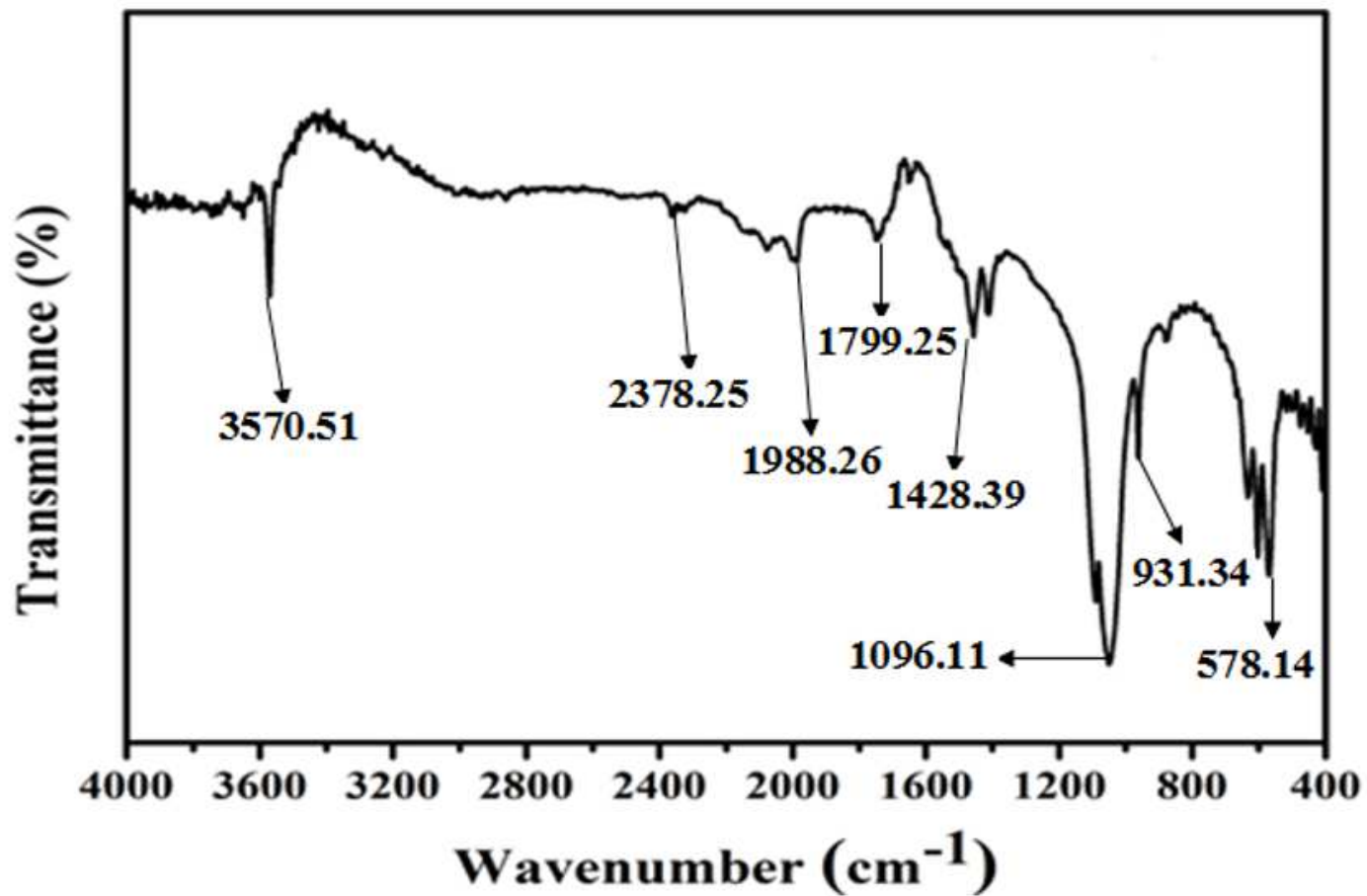


Figure 4

FTIR Spectrum of K- - SC1.5

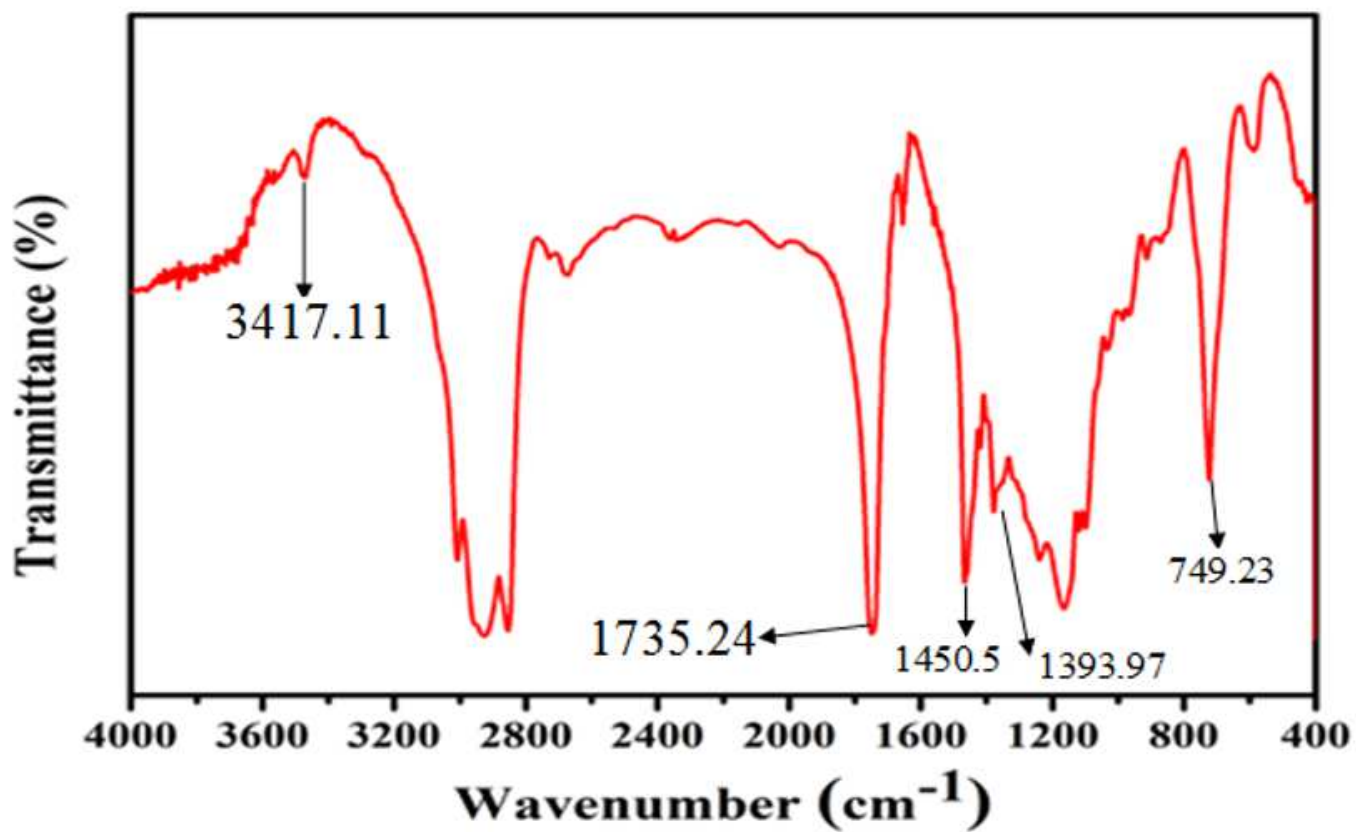


Figure 5

FTIR spectrum for biodiesel produced from K- - SC1.5 at 65°C after 2.5h

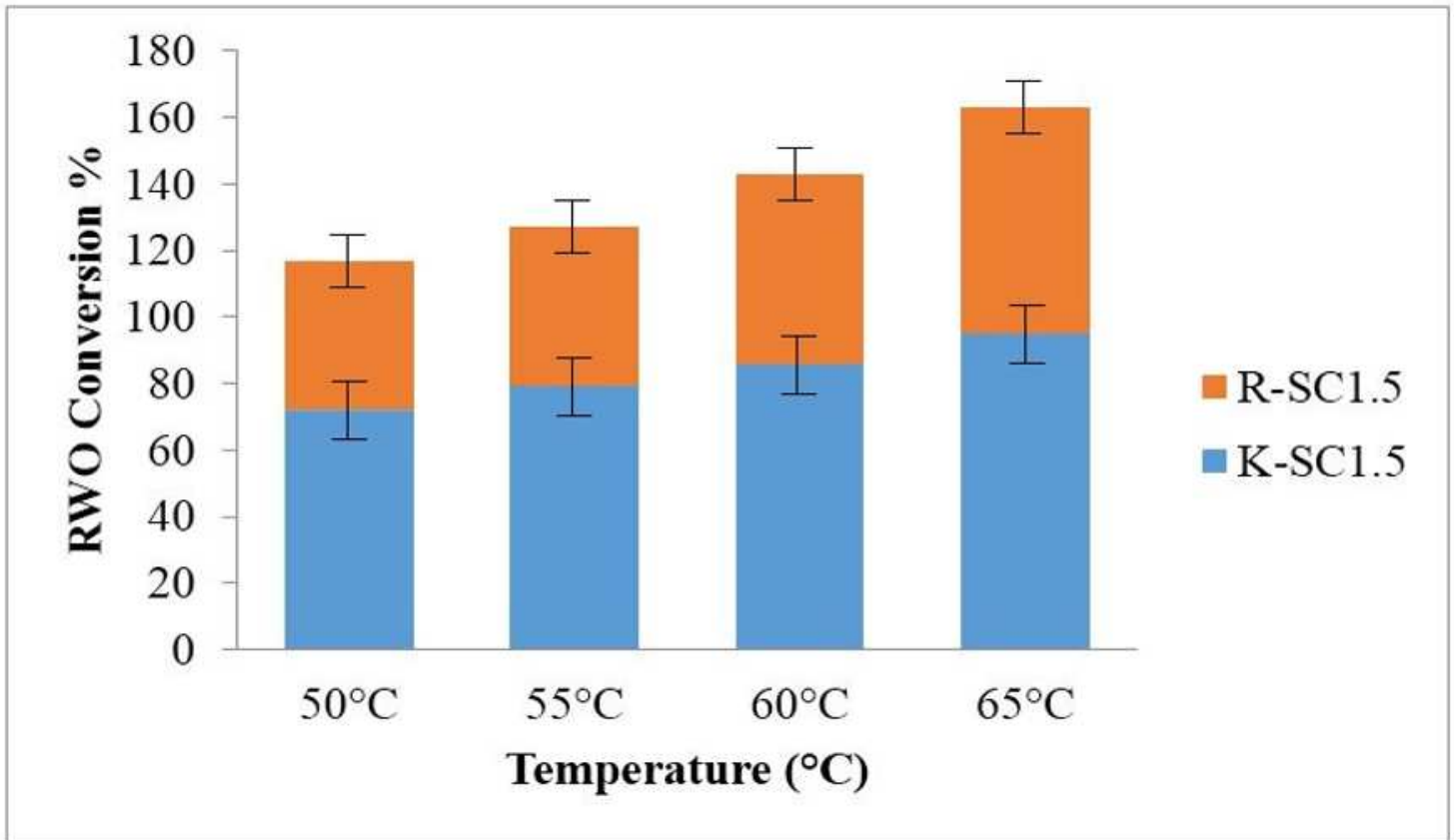


Figure 6

Maximum biodiesel conversion for R - SC1.5 and K- - SC1.5 after 2.5h

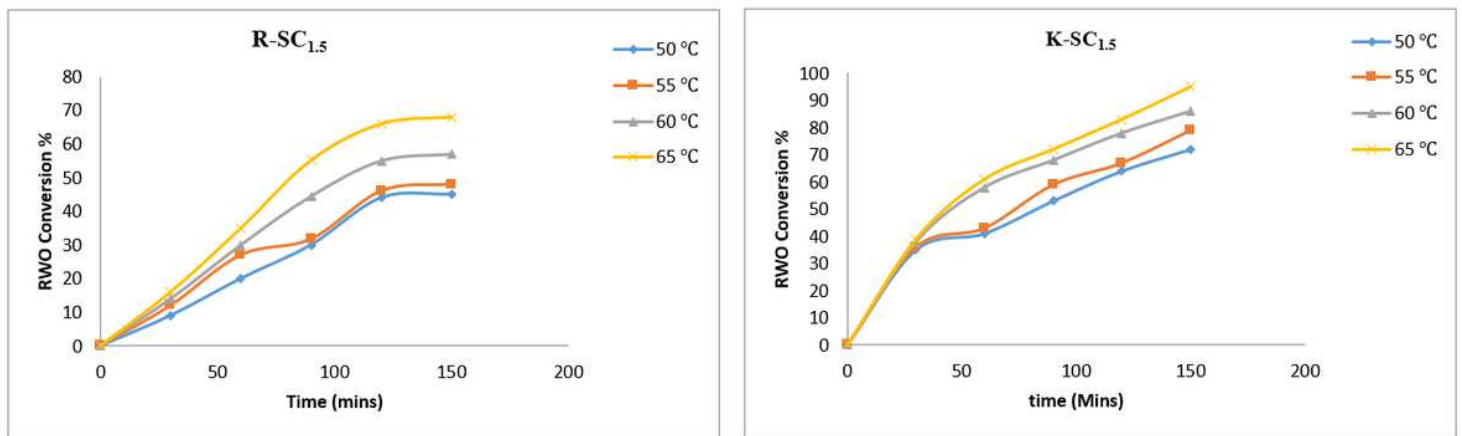


Figure 7

a Effect of temperature and time of RWO conversion (R-SC1.5) b Effect of temperature and time of RWO conversion (K-SC1.5)

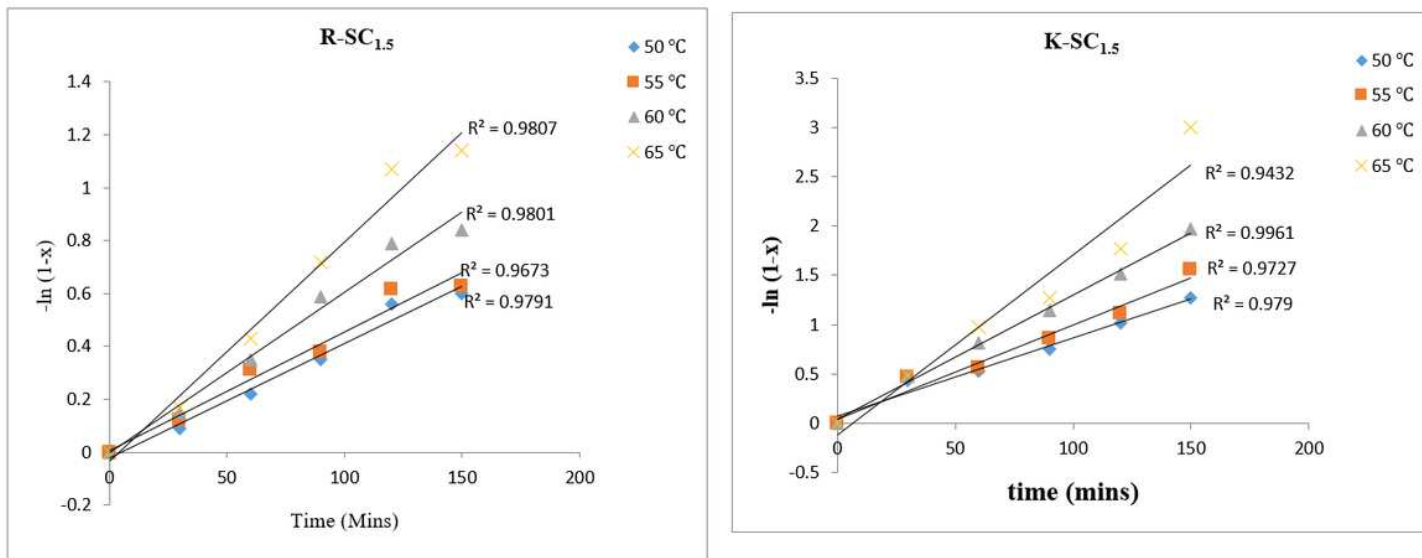


Figure 8

plot of $-\ln(1-X)$ against t

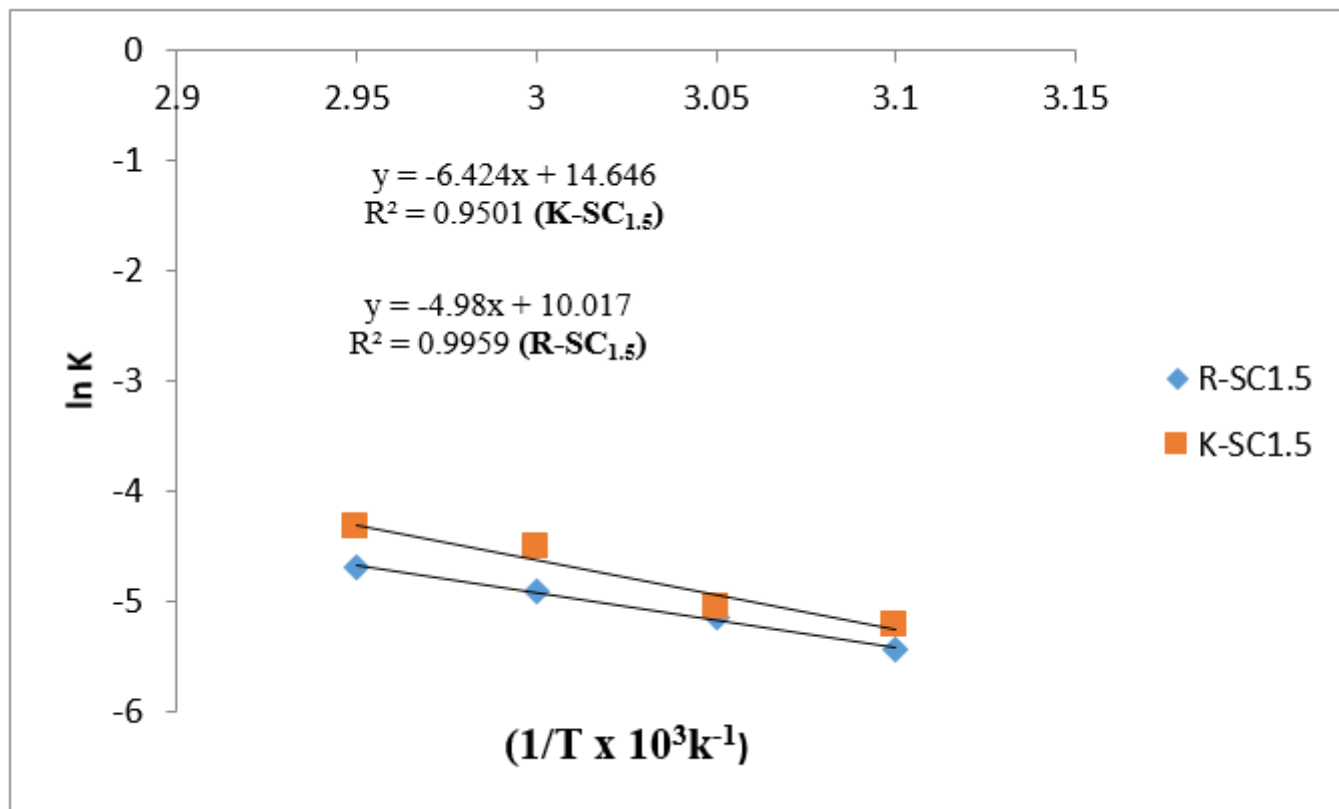


Figure 9

Plot of $\ln K$ against $1/T \times 10^{-3}$ (R-SC1.5 and K-SC1.5)

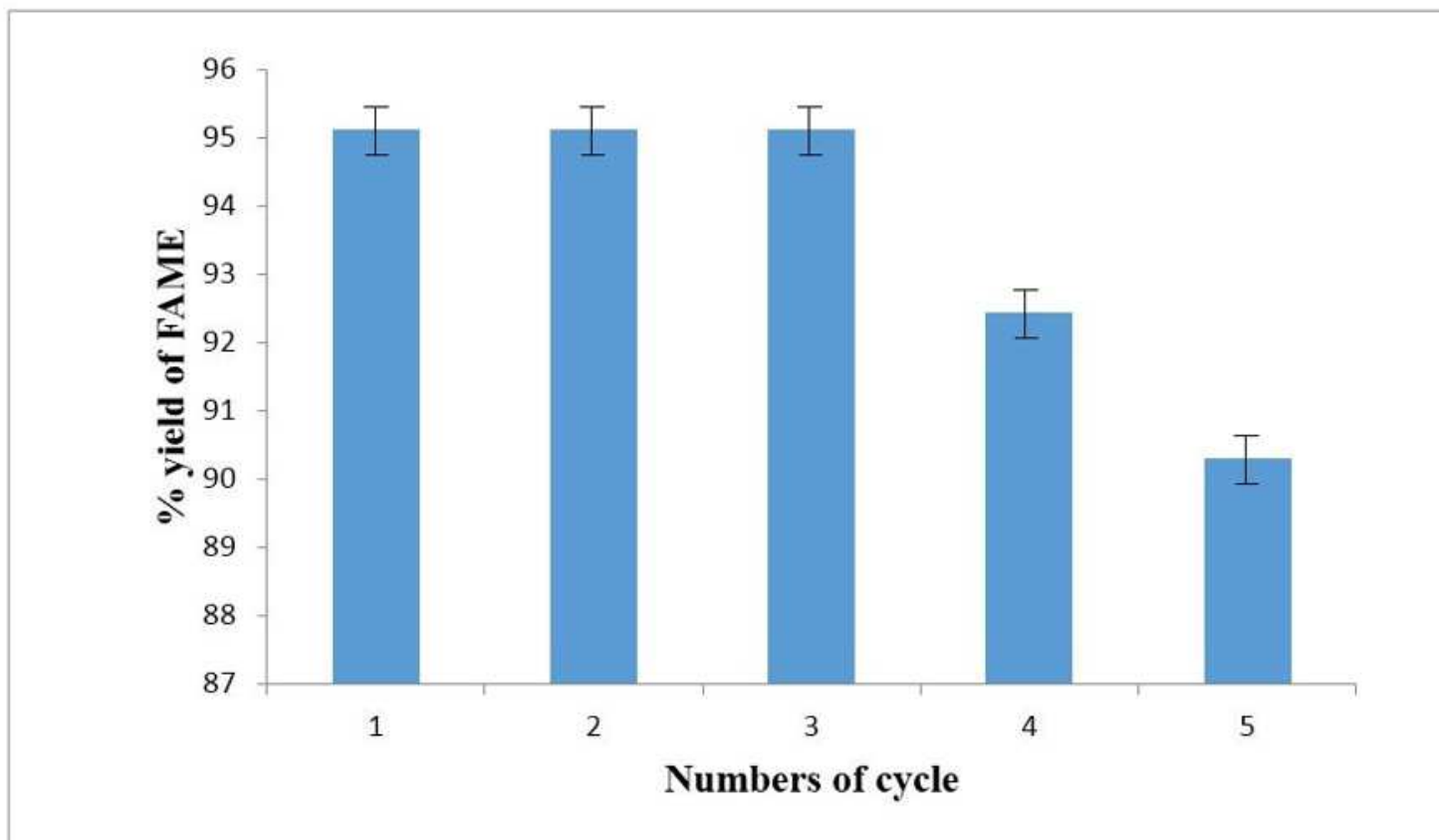


Figure 10

Reusability study of K-SC1.5 catalyst